

# Ingress of NaCl in concrete with alkali reactive aggregate: effect on silicon solubility

Anne Heisig · Liudvikas Urbonas ·  
Robin E. Beddoe · Detlef Heinz

Received: 16 October 2015 / Accepted: 25 December 2015 / Published online: 4 January 2016  
© RILEM 2016

**Abstract** Enhanced damage due to the alkali–silica reaction (ASR) in concrete exposed to deicing salt (NaCl) is usually attributed to binding of chloride ions in the hydration products of cement. To balance charge,  $\text{OH}^-$  ions are released into the concrete pore solution which increases alkalinity. However, during NaCl ingress a decrease in the  $\text{OH}^-$  concentration of the concrete pore solution due to potassium leaching would reduce  $\text{SiO}_2$  solubility and therefore ASR damage. The present work combines expansion measurements with pore solution analysis by ICP-OES and XRD measurements on concretes and hydrated cement pastes. Solubility equilibria calculations were performed with the hydrogeochemical simulation program PHREEQC. The investigations show that the  $\text{OH}^-$  concentration of the pore solution is mainly lowered by potassium leaching during NaCl ingress. The  $\text{OH}^-$  concentration also decreases owing to the formation of Friedel’s salt from ettringite which is associated with the release of sulphate. Although the  $\text{OH}^-$  concentration with NaCl is lower, ASR damage is intensified and the silicon concentration in the pore solution is higher. Higher silicon solubility is explained by the higher total alkali concentration

which increases surface silicate solubility, the formation of an aqueous complex  $\text{NaHSiO}_3^0$  and a higher ionic strength. These effects promote the sensitivity of silicate minerals to ASR, the formation of alkali silica gel and finally ASR damage.

**Keywords** Alkali–silica reaction ·  $\text{OH}^-$  concentration · Pore solution ·  $\text{SiO}_2$  solubility

## Abbreviations

ASR	Alkali–silica reaction
HA	Cement with a high alkali equivalent
LA	Cement with a low alkali equivalent
$\text{Na}_2\text{O}_{\text{eq}}$	Alkali equivalent
ICP-OES	Inductively Coupled Plasma Optical Emission Spectrometry
XRD	X-ray diffraction
PHREEQC	Computer program for hydrogeochemical simulations
WATEQ	Activity calculation of species
LLNL	Database

## 1 Introduction

In recent years, cracks were often observed in German motorway pavement and other concrete structures exposed to deicing salt [1]. Investigations of the

A. Heisig (✉) · L. Urbonas · R. E. Beddoe · D. Heinz  
Chair of Mineral Engineering, Technische Universität  
München, Baumbachstraße 7, 81245 Munich, Germany  
e-mail: anne.heisig@tum.de  
URL: <http://www.cbm.bgu.tum.de>

concrete revealed the presence of alkali silica gel in the cracked concrete indicating the occurrence of a damaging alkali–silica reaction [2]. The enhancement of ASR damage in concrete structures and pavement exposed to deicing salt has also been observed in many other countries and has been the subject of numerous laboratory and field investigations [3–11].

To investigate the effect of alkali ingress on concrete expansion, Chatterji et al. [4] measured the expansion of mortar prisms ( $4 \times 4 \times 16 \text{ cm}^3$ ) made with highly reactive sand during storage at  $50^\circ \text{C}$  in 3 mol/L NaOH or in NaCl solutions with different concentrations (3, 2, 1 and 0.5 mol/L). During the first weeks, the specimens stored in the NaOH solution exhibited the larger expansion. However, after about 9 weeks, the expansion of the specimens in the NaCl solutions was considerably higher. Moreover, with increasing NaCl concentration (from 0.5 to 2 mol/L), the expansion began earlier and the final expansion after 56 weeks was higher.

In investigations with concrete structures and laboratory concretes, Sibbick and Page [8, 9] assessed the effect of NaCl exposure on ASR in concrete with regard to the alkali content of the concrete and the  $\text{C}_3\text{A}$  content of the cement. The authors proposed a reaction scheme in which, firstly, the ingress of NaCl increases the NaOH concentration of the pore solution owing to the reaction of chloride with the  $\text{C}_3\text{A}$  hydration products and portlandite. Secondly, the increase in  $\text{OH}^-$  concentration promotes the neutralization of the acidic silanol groups ( $\equiv \text{SiOH}$ ) at the  $\text{SiO}_2$  surface and thus the formation of negatively charged  $\equiv \text{SiO}^-$  surfaces.

It is well known that the dissolution of silica, i.e.  $\text{SiO}_2$ , is controlled by the concentration of  $\text{OH}^-$  ions because this changes the solubility equilibrium between solid  $\text{SiO}_2$  and the aqueous  $\text{H}_4\text{SiO}_4^0$  species. At pH above 11,  $\text{H}_4\text{SiO}_4^0$  exists with an increasing amount of its deprotonated forms causing more  $\text{SiO}_2$  to dissolve. Cations, e.g.  $\text{Na}^+$ ,  $\text{K}^+$  or  $\text{Ca}^{2+}$ , are preferentially bound at the negative surface sites. The  $\text{SiO}_2$  network disintegrates forming a loose gel structure [5, 12]. According to the reaction scheme of Sibbick and Page [8, 9] a fluid alkali-rich silica gel is formed which takes up calcium and water and is able to develop an expansion pressure.

In other laboratory and field investigations, Bérubé et al. [3] estimated the effect of NaCl ingress on ASR with regard to the alkali content and

thickness of the specimens. Exposure of concrete to NaCl solutions was found to result in an increase in sodium and chloride concentration in the concrete. At the same time the potassium and the calculated  $\text{OH}^-$  concentrations decreased owing to leaching of the near-surface concrete layers. Thus the pH of the concrete pore solution was lower in the regions affected by NaCl ingress. Based on these results, the authors suggest that ASR damage in thin structures is reduced by leaching. In thick structures, the effect of NaCl is limited by its penetration depth. If the concrete contains high-alkali cements, ASR takes place in the inner, unaffected region as usual, i.e. is not affected by the external alkalis. In this case the formation of a swelling alkali silica gel inside the concrete leads to inhomogeneous expansion which induces cracks.

However, the effect of NaCl ingress on the composition of the concrete pore solution and the dissolution rate of  $\text{SiO}_2$  was not considered in the laboratory and field investigations mentioned above [3, 4, 8, 9]. According to Bérubé et al. [3], leaching of potassium during exposure of concrete to NaCl solutions results in a reduction in pH of the concrete pore solution,  $\text{SiO}_2$  solubility and consequently less ASR damage. Nevertheless, as described previously [4–11], NaCl ingress in hardened concrete can promote damage due to ASR significantly. Moreover, NaCl increases capillary porosity which accelerates transport [13, 14] and also affects the phase composition of the hydration products [8, 9, 15] as well as, in particular, the composition of the pore solution [15]. It is often assumed that during chloride binding the negative charge of the chloride ions is compensated by the release of  $\text{OH}^-$  ions into the pore solution. This would mean an increase in the pH of the concrete pore solution and consequently more ASR damage [9, 16–19]. In contrast, Chatterji et al. [4, 20] suggested that alkali salts can directly participate in the ASR and that chloride binding is not relevant for damaging ASR.

Although the mechanisms responsible for ASR are well understood, there are conflicting interpretations on how ASR proceeds in presence of NaCl. This paper considers the changes in the pore solution and cement hydration phases caused by NaCl ingress in concrete and its effect on the solubility of silicon in borosilicate glass as a model for reactive aggregate in concrete.



## 2 Materials and methods

### 2.1 Materials and specimen preparation

Two Portland cements CEM I 32.5 R were used representing cements with high (HA) and low (LA) alkali equivalents, i.e. 1.02 and 0.56 wt%  $\text{Na}_2\text{O}_{\text{eq}}$ , respectively (Table 1).

For expansion measurements, concrete bars ( $40 \times 40 \times 160 \text{ mm}^3$ ) were produced with end gauge marks using aggregate composed of 45 vol% ( $=660 \text{ kg/m}^3$ ) borosilicate glass (fraction 2/8 mm) as a model reactive aggregate [21, 22] with a homogeneous composition (Table 2), 5 vol% inert diabase (fraction 2/8 mm) and 50 vol% inert quartz sand (fraction 0/2 mm). The concretes were produced with  $400 \text{ kg/m}^3$  cement and a  $w/c$  ratio of 0.5.

Experiments were also performed with finely ground hardened cement paste (i.e. without reactive aggregate) stored in an artificial pore solution in order to investigate the chemical balance between the pore solution and the solid phases while minimizing the effect of transport (porosity) and leaching. Cement pastes of the same composition ( $w/c = 0.5$ ) were mixed and poured into PE bottles which were sealed and rotated for 24 h to prevent segregation. The pastes were stored in the bottles up to an age of 91 days at

20 °C. Pore solutions were then expressed (Table 3, left) and powder specimens produced by grinding of the solid material for 60 s in isopropanol in a disc mill and then drying at 40 °C for about 2 h. The hydrated cement paste powders were stored for 14 days at 20 °C under rotation in artificial pore solutions (Table 3, right), water/solid ratio  $w/s = 1$ , corresponding to the expressed pore solution of the particular hydrated cement. This procedure was necessary to ensure hydration of the freshly fractured surface of the residual clinker phases produced during grinding. The amount of water bound in hydrates was then compensated by adjusting the  $w/s$  back to 1. Afterwards artificial pore solution was added to increase the  $w/s$  ratio to 2:1. Different amounts of finely ground NaCl were then added to the solutions to produce concentrations of 0, 3, 10 and 20 wt% NaCl.

### 2.2 Expansion measurements

The concrete bars were cast for each particular cement, demoulded after 24 h and also stored at 20 °C in moist air (over water) for a period of 91 days (pre-storage). Afterwards, the bars were stored in moist air or a 20 wt% NaCl solution for 274 days (age: 1 year) at 20 °C. The ratio of solution to specimen volume was  $2 \pm 0.5$ .

**Table 1** Alkali content (left) and mineralogical composition (right) of the cements, wt%

CEM I 32.5 R	Chemical analysis <sup>a</sup>			X-ray diffraction (XRD) <sup>b</sup>				
	K <sub>2</sub> O	Na <sub>2</sub> O	Na <sub>2</sub> O <sub>eq</sub> <sup>c</sup>	CaCO <sub>3</sub>	C <sub>3</sub> S	C <sub>2</sub> S	C <sub>3</sub> A	C <sub>4</sub> AF
HA	1.20	0.24	1.02	4.86	56.64	11.32	6.63	12.68
LA	0.46	0.26	0.56	5.25	45.68	23.75	8.70	8.79

<sup>a</sup> Extraction with lithium metaborate, ICP-OES

<sup>b</sup> With Rietveld refinement

<sup>c</sup> Alkali equivalent:  $\text{Na}_2\text{O}_{\text{eq}} = \text{Na}_2\text{O} + 0.658 \text{ K}_2\text{O}$

**Table 2** Chemical composition<sup>a</sup> of the borosilicate glass, wt%

Borosilicate glass								
SiO <sub>2</sub>	B <sub>2</sub> O <sub>3</sub> <sup>b</sup>	Al <sub>2</sub> O <sub>3</sub>	Fe <sub>2</sub> O <sub>3</sub>	CaO	P <sub>2</sub> O <sub>5</sub>	K <sub>2</sub> O	Na <sub>2</sub> O	Na <sub>2</sub> O <sub>eq</sub> <sup>c</sup>
82.04	12.52	2.58	0.32	0.13	0.14	0.65	3.41	3.84

<sup>a</sup> Extraction with lithium metaborate, ICP-OES

<sup>b</sup> Digestion in fused NaOH, ICP-OES

<sup>c</sup> Alkali equivalent:  $\text{Na}_2\text{O}_{\text{eq}} = \text{Na}_2\text{O} + 0.658 \text{ K}_2\text{O}$



**Table 3** Chemical composition of the pore solutions of the hardened cement pastes after 91 days hydration at 20 °C (left) and weights of compounds for the production of the corresponding artificial pore solutions (right)

Component (mmol/L)	CEM I 32.5 R		Material (g/L)	CEM I 32.5 R	
	HA <i>w/c</i> = 0.50	LA		HA <i>w/c</i> = 0.50	LA
OH <sup>-a</sup>	611.4	338.5	Ca(OH) <sub>2</sub>	– <sup>c</sup>	
CaO	1.3	1.9	NaOH	21.78	28.80
Na <sub>2</sub> O	125.9	134.4	KOH	135.03	54.56
K <sub>2</sub> O	514.1	200.2	K <sub>2</sub> SO <sub>4</sub>	12.60	2.23
SiO <sub>2</sub>	0.6	0.5	KCl	1.42	0.23
Al <sub>2</sub> O <sub>3</sub>	0.1	0.1	Na <sub>2</sub> SiO <sub>3</sub> ·5H <sub>2</sub> O	0.66	0.55
Cl <sup>-b</sup>	19.9	1.6	NaCl	4.61	0.20
SO <sub>4</sub> <sup>2-</sup>	14.5	2.6	AlCl <sub>3</sub> ·6H <sub>2</sub> O	0.12	0.10

<sup>a</sup> By titration (indicator: toluene red)

<sup>b</sup> Photometric analysis

<sup>c</sup> Supplied by dissolution of binder during storage for ease of preparation

Changes in the length and mass of the bars were recorded during the moist pre-storage at ages of 1, 28, 91 days and thereafter every four weeks.

### 2.3 Pore solution analysis

Pore solutions were expressed at high pressure (500 MPa) from the concrete bars at ages of 91 (i.e. immediately after pre-storage), 231 days and 1 year.

Pore solutions were also expressed from the hardened pastes at an age of 91 days and the chemical composition determined (Table 3, left).

After a storage period of 28 days under rotation the suspensions of the hydrated cement paste powders and the artificial pore solution were centrifuged, the solutions filtered and the filtrate composition determined. The solid material was dried at 40 °C and investigated by X-ray diffraction.

The chemical composition of all the solutions was analysed by ICP-OES as well as photometry and the pH determined by titration.

### 2.4 X-ray diffraction (XRD)

For the X-ray investigations the hydrated cement paste powder was finely ground for five minutes in isopropyl alcohol in a laboratory ball mill and then dried at 40 °C for 30 min. The specimens were stored in an argon atmosphere until measurement. The XRD measurements were performed with a XRD 3003 TT

diffractometer of GE Sensing & Inspection Technologies GmbH with  $\theta$ – $\theta$  configuration und CuK <sub>$\alpha$</sub>  radiation ( $\lambda = 1.54 \text{ \AA}$ ). Intensities were recorded over scattering angles of 5–70° 2 $\theta$  with a step width of 0.02° and a measuring time of 6 s/step.

## 3 Results and discussion

### 3.1 Concrete specimens

As expected, the expansion of the prisms with the high alkali cement during moist storage is significantly larger (Fig. 1): 3.59 mm/m for concrete with cement HA and 1.46 mm/m with the low-alkali cement LA after 1 year. The expansion rate of the bars with the high alkali cement during moist storage is significantly faster. The onset of internal damage was characterized by the reduction in the frequency of resonance (arrows) of the specimens. The specimens with the LA cement were not damaged by ASR after 1 year storage whereas the specimens with the HA cement were. The ASR expansion of the specimens made with HA cement is obviously derived from the alkalis in this cement.

The effect of cement alkali content on the expansion of the concretes during subsequent NaCl exposure is shown in Fig. 2 for up to an age of 1 year. In the pre-storage period, the expansion of specimen HA is 2.6 times more than that of specimen LA. During



subsequent NaCl exposure, the expansion of the bars with HA and LA cement increased up to 6.11 and 4.33 mm/m, respectively, over a period of 274 days.

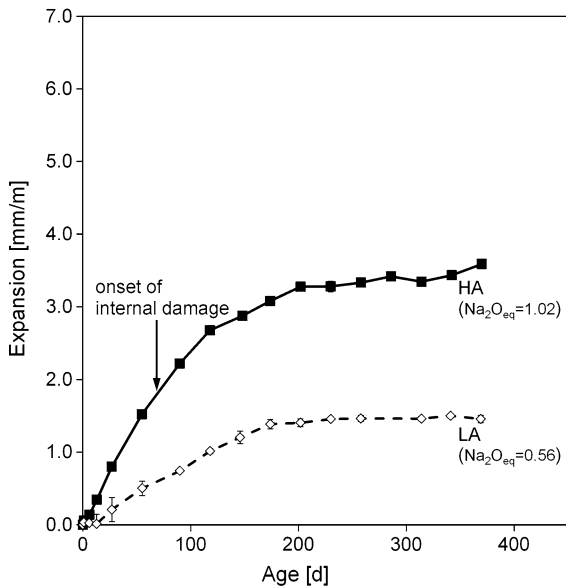


**Fig. 1** Expansion of concrete bars (average over three specimens, error bars often smaller than symbols) with borosilicate glass for high and low alkali cements during moist storage at 20 °C

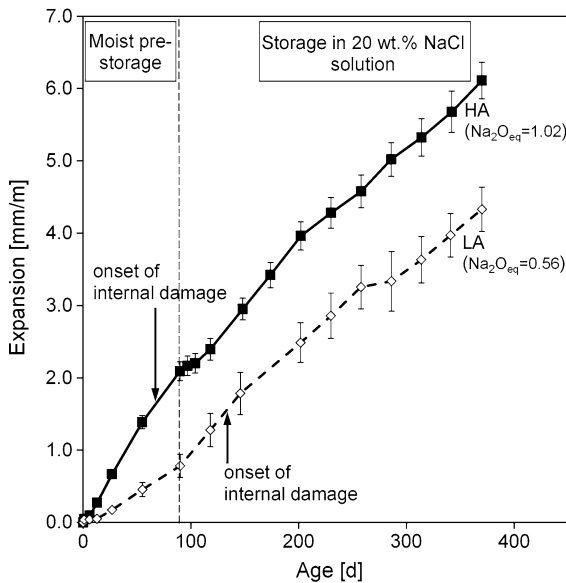


**Fig. 2** Expansion of concrete bars (average over three specimens) with borosilicate glass for high and low alkali cements during 91 days moist pre-storage and subsequent 274 days storage in 20 wt% NaCl solution at 20 °C

The rates of expansion of specimens HA and LA during subsequent storage in NaCl solution are similar (HA is 1.1 times faster than LA) for both concretes, i.e. 4.02 and 3.55 mm/m over 274 days, for HA and LA cement, respectively. The concrete made with LA cement expanded rapidly with an onset of internal damage between 118 and 140 days. In view of the low alkali content of the cement, this behaviour can only be explained by ASR due to NaCl ingress.

Figure 3 shows the mass change of the specimens during NaCl storage. Since the change in mass of the concretes produced by the uptake of storage solution is similar, it may be assumed that the ingress of NaCl is also similar. These results indicate that the alkali content of the cement is no longer decisive for damaging ASR in concrete exposed to external alkalis, i.e. low alkali cements in concrete exposed to deicing salt do not always prevent ASR damage as also observed by other authors [23, 24]. Similar results were obtained in earlier experiments by the present author [25] in a performance test including NaCl ingress. Different concrete compositions with natural alkali reactive aggregates, e.g. Precambrian greywacke or reactive crushed material originating from the upper Rhine Valley were considered.

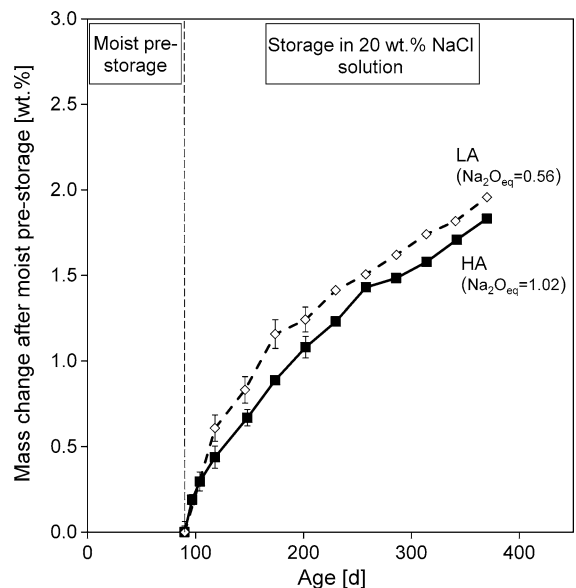


**Fig. 3** Increase in mass of concrete bars (average over three specimens, error bars often smaller than symbols) with borosilicate glass for high and low alkali cements after pre-storage and subsequent storage in 20 wt% NaCl solution at 20 °C

Opposed to the present observations, investigations with laboratory and field concretes by Bérubé et al. [3] show no effect of external alkalis on ASR in concrete with low-alkali cement. As mentioned above, the authors suggest that ASR in near surface layer is reduced owing to low  $\text{OH}^-$  concentrations produced by potassium leaching although sodium and chloride are present. ASR in deeper layers is, as would be expected, not affected by leaching and chloride ingress. The disagreement with the present observations for low-alkali cement may originate in the different storage conditions (temperature and chloride concentration) and specimen geometry.

The results of the pore solution analysis after different storage periods reveal a decrease in both  $\text{OH}^-$  (Fig. 4) and potassium concentration (Fig. 5) and an increase of sulphate concentration (Fig. 4) in both concretes.

In the case of ASR without external alkali exposure, the hydroxide ion concentration is approximated by the total alkali concentration, i.e.  $[\text{OH}^-] \approx [\text{Na}^+] + [\text{K}^+]$  [26]. Due to the ingress of external alkalis (NaCl) combined with an enrichment of sodium and chloride ions in the pore solution a strong shift occurs towards the negative charged ions. In this case the approximation is  $[\text{Na}^+] + [\text{K}^+] \approx [\text{OH}^-] + [\text{SO}_4^{2-}] + [\text{Cl}^-]$ .

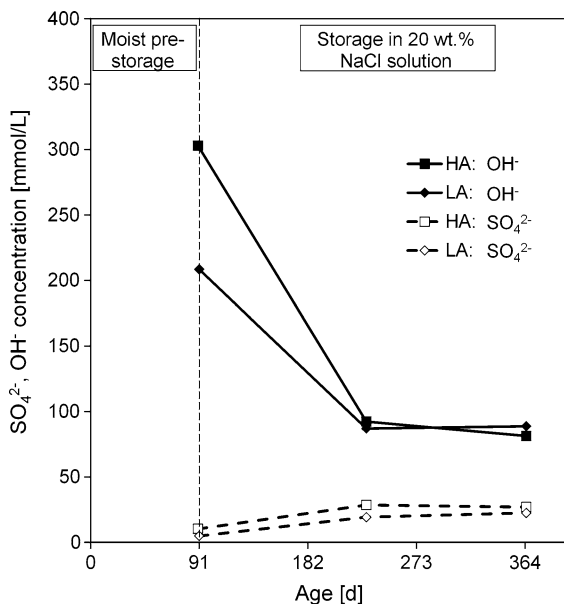


**Fig. 4**  $\text{OH}^-$  and  $\text{SO}_4^{2-}$  concentration in the pore solution of concretes with borosilicate glass stored in 20 wt% NaCl solution for high and low alkali cements

As expected, the pore solution of the concrete with low alkali cement has a lower  $\text{OH}^-$  concentration at the end of the moist pre-storage (91 days). During the following storage in 20 wt% NaCl solution, the  $\text{OH}^-$  concentration in both concretes drops to a minimum of about 85 mmol/L (pH 12.9) irrespective of the initial alkalinity of the pore solution (Fig. 4). Figure 5 also shows the total alkali concentrations (Na + K) after 91 days moist pre-storage. These values are in agreement with the corresponding  $\text{OH}^-$  concentrations in Fig. 4.

Changes in the  $\text{OH}^-$  concentration of the pore solution may be explained by the following mechanisms.

- A decrease due to diffusion of potassium ions into the storage solution (leaching).
- A decrease due to the binding of alkalis (Na and K) in alkali silica gel.
- An increase due to chloride binding in the hydration products.
- A decrease due to sulphate release into the pore solution and the corresponding charge balance.

Measurements of ASR gels formed in the present concrete bars show that the gel structure usually

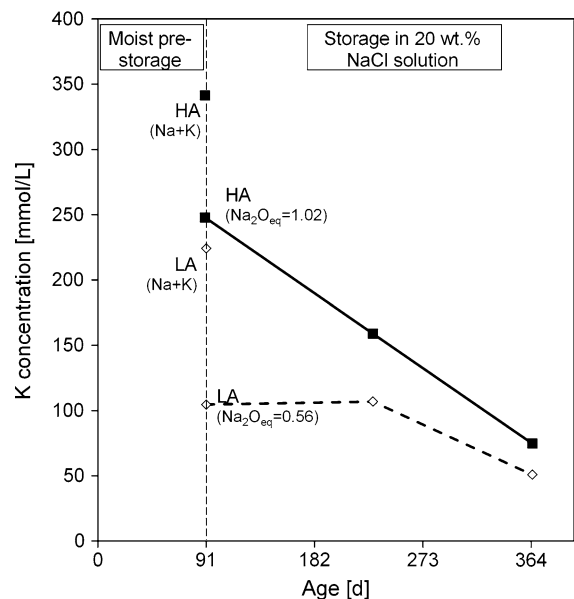


**Fig. 5** K concentration in the pore solution of concretes with borosilicate glass stored in 20 wt% NaCl solution for high and low alkali cements. The symbols labelled (Na + K) represent the total alkali concentration after 91 days moist pre-storage

contains small amount potassium (around 2 %) as opposed to sodium (around 20 %). Thus it is apparent that the loss in alkalinity in Fig. 5 is mainly due to potassium leaching into the external storage solution against the flux of sodium and chloride ions into the concrete specimens (Fig. 6).

As expected, the concentrations of sodium and, correspondingly, chloride increase with the duration of NaCl exposure (Fig. 6) as sodium and chloride ion diffuse into the concrete. Concentrations close to the external storage solution were reached over a period of 274 days (age: 1 year). Despite the continuous reduction in  $\text{OH}^-$  concentration during storage, the concentration of silicon in fact increases (Fig. 7). This enhanced silicon solubility can only be explained by the high concentrations of sodium and chloride ions which outweigh the effect of the pH reduction due to potassium leaching. This effect is confirmed by the investigations of Dove and Elston [27] who considered the solubility of quartz in different NaCl solutions. The solubility of silicon was found to increase in the presence of NaCl, see details in Sect. 3.3.

Similar changes in pore solution composition were observed by the present author in earlier experiments with concretes containing natural aggregates [25].

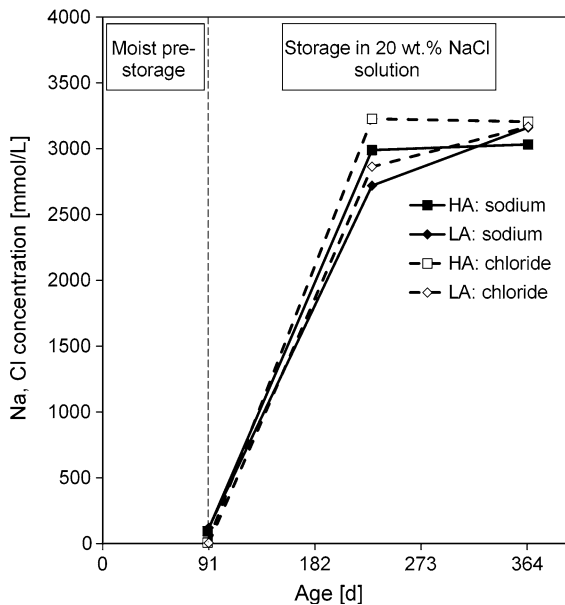


**Fig. 6** Na and Cl concentration in the pore solution of concretes with borosilicate glass stored at 20 °C in 20 wt% NaCl solution for high and low alkali cements

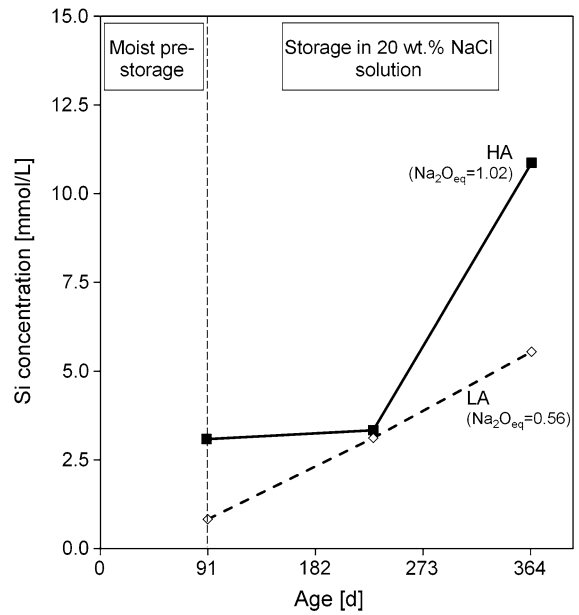


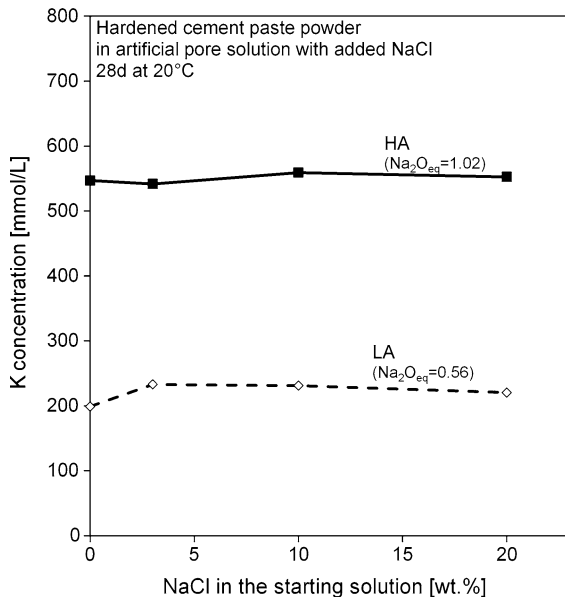
**Fig. 7** Si concentration in the pore solution of concretes with borosilicate glass stored at 20 °C in 20 wt% NaCl solution for high and low alkali cements

### 3.2 Hydrated cement paste powder

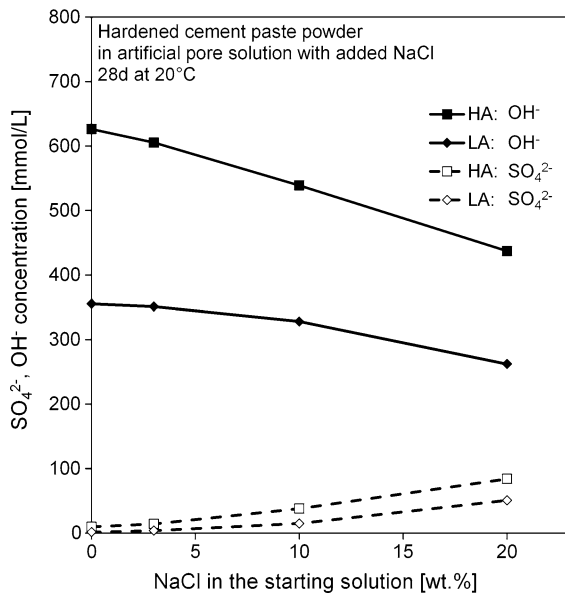
The results of the storage experiments with hydrated cement paste powder in artificial pore solutions are presented in Figs. 8 and 9. Like the concrete, the NaCl storage started at an age of 91 days, but was terminated after 28 days when equilibrium between cement phases and pore solution was reached. Owing to the use of pure cement paste powders and the appropriate artificial pore solution, the effect of potassium leaching as well as alkali binding by ASR gel formation on the  $\text{OH}^-$  concentration were eliminated in these experiments. Transport effects are minimized as well owing to the use of finely ground, hydrated cement paste powder ( $<63 \mu\text{m}$ ).

Figure 8 shows the potassium concentration in the artificial pore solution for increasing amounts of NaCl. The concentration is constant because in these experiments leaching was excluded. Nevertheless, the  $\text{OH}^-$  concentration clearly decreases when more NaCl is added to the initial storage solution (Fig. 9). At the same time, the concentration of sulphate increases maintaining constant negative charge with the  $\text{OH}^-$  ions.

According to the XRD measurements with the powder specimens Friedel's salt is formed consuming AFm (monocarbonate) and AFt (ettringite) phases of the hydrated cements (Figs. 10, 11).



**Fig. 8** Effect of addition of NaCl on the K concentration of the artificial pore solution after 28 days storage of hydrated cement paste powder for high and low alkali cements



**Fig. 9** Effect of addition of NaCl on the OH<sup>-</sup> and SO<sub>4</sub><sup>2-</sup> concentration of the artificial pore solution after 28 days storage of hydrated cement paste powder for high and low alkali cements

The increase in sulphate concentration in Fig. 9 is due to the reaction of chloride with ettringite (3CaO·Al<sub>2</sub>O<sub>3</sub>·3CaSO<sub>4</sub>·32H<sub>2</sub>O) resulting in the formation

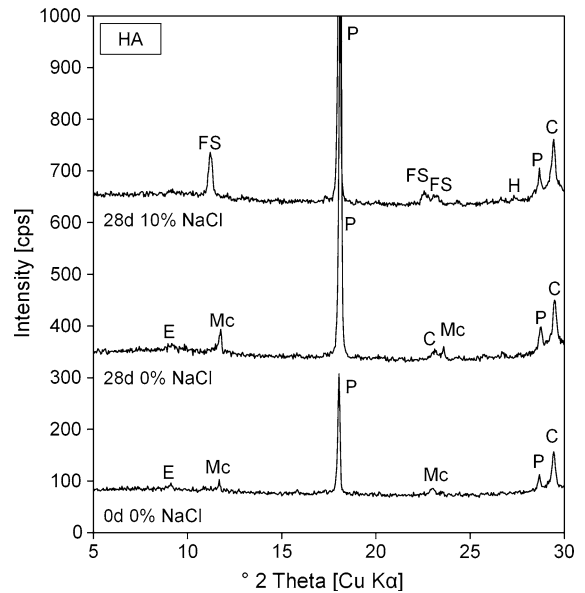
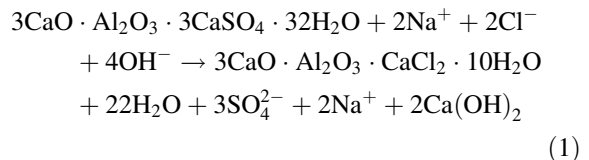
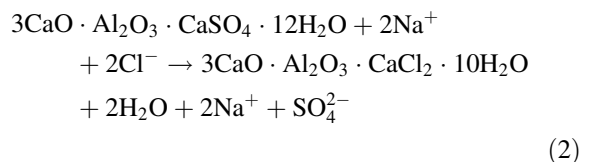


**Fig. 10** Effect of addition of 10 wt% NaCl to the artificial pore solution on the phase composition of the hydrated cement paste powder for cement HA (CEM I 32.5 R, Na<sub>2</sub>O<sub>eq</sub> = 1.02 wt%): C calcite, E ettringite, FS Friedel's salt, H halite, Mc monocarbonate, P portlandite

of Friedel's salt (3CaO·Al<sub>2</sub>O<sub>3</sub>·CaCl<sub>2</sub>·10H<sub>2</sub>O) and release of sulphate ions (Eq. 1). The available phases and solution pH are favourable for the formation of Friedel's salt.



Monosulphate (3CaO·Al<sub>2</sub>O<sub>3</sub>·CaSO<sub>4</sub>·12H<sub>2</sub>O) was not detected by XRD in this investigation, but this phase also releases sulphate on forming Friedel's salt (Eq. 2) [28].



The formation of Friedel's salt also results in a change of pH of the pore solution depending on the phase participating in the reaction with NaCl. In case of ettringite, the pH is lowered owing to the formation of portlandite (Ca(OH)<sub>2</sub>) (Eq. 1). Monosulphate transformation has no effect on pH (Eq. 2), but AFm



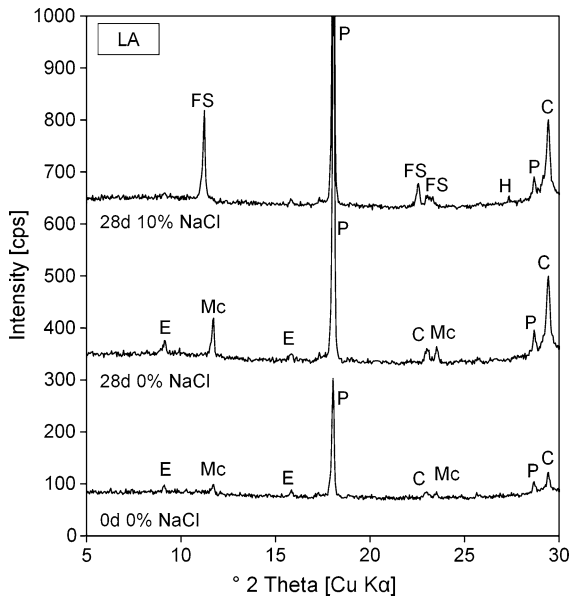
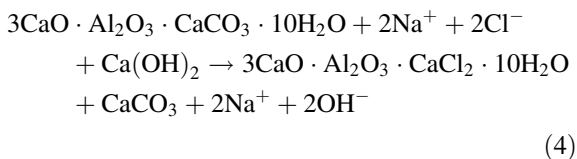
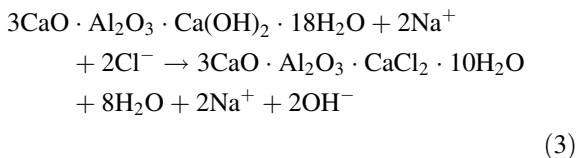


**Fig. 11** Effect of addition of 10 wt% NaCl to the artificial pore solution on the phase composition of the hydrated cement paste powder for cement LA (CEM I 32.5 R,  $\text{Na}_2\text{O}_{\text{eq}} = 0.56$  wt%): C calcite, E ettringite, FS Friedel's salt, H halite, Mc monocarbonate, P portlandite

containing hydroxide ( $3\text{CaO} \cdot \text{Al}_2\text{O}_3 \cdot \text{Ca}(\text{OH})_2 \cdot 18\text{H}_2\text{O}$ ) (Eq. 3) or carbonate ( $3\text{CaO} \cdot \text{Al}_2\text{O}_3 \cdot \text{CaCO}_3 \cdot 10\text{H}_2\text{O}$ ) (Eq. 4) can increase the pH of the pore solution. Calcite forms owing to the transformation of monocarbonate to Friedel's salt (Eq. 4).



The pore solution analysis and XRD results indicate that the decrease in pH and increase in sulphate concentration observed for the cements HA and LA are mainly due to the transformation of ettringite to Friedel's salt. Similar changes in  $\text{OH}^-$  and  $\text{SO}_4^{2-}$  concentration were also observed in earlier experiments [25] for the pore solutions expressed from concrete specimens made with the same cements (Figs. 4, 9) and using natural aggregates.

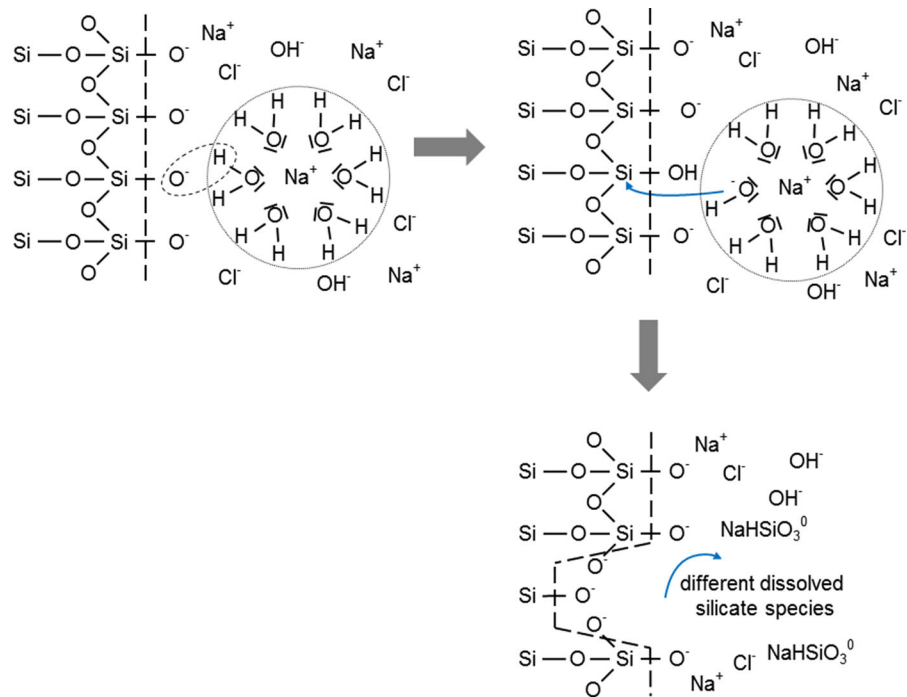
The concentration of  $\text{OH}^-$  in the storage solution of the powder specimens (91 days sealed storage and 28 days in artificial pore solution) is generally higher (Fig. 9) than that of the concretes after 91 days moist storage (Fig. 4). Although the absolute concentrations in the artificial and concrete pore solutions differ, the general trends are similar. This difference is due to, for example, alkali consumption of the reaction products of ASR [5], different storage conditions (e.g. pre-storage sealed or over water, leaching effects, prism sizes, [29, 30]), amount of water in contact with solids (solution to solid ratio) etc.

### 3.3 Solubility calculations

Owing to the effects considered above, the  $\text{OH}^-$  concentration in the pore solution of the concretes drops to values below 100 mmol/L (<pH 13.0) after 231 days storage in 20 wt% NaCl solution (Fig. 4). As a result, damaging ASR should, in theory, cease [31, 32] because the necessary  $\text{OH}^-$  concentration for high silicon solubility and alkali silica gel formation is no longer reached. However, the above results show that exposure to NaCl increases the solubility of silicon in siliceous aggregate and therefore ASR expansion and damage significantly. This indicates that the promotion of ASR in the presence of externally supplied alkalis is linked to the increase in sodium chloride concentration in the pore solution by mechanisms other than the effect of pH on aggregate solubility. In particular, the expansion of the concrete with the low-alkali cement is accelerated markedly (65 % more expansion in comparison to the pre-storage) in the presence of external alkalis. As mentioned above, this confirms the results of other authors [23, 24] showing that low-alkali cements cannot in all cases inhibit damaging ASR in concrete exposed to deicing salt.

Dove and Elston [27] considered the effect of dissolved sodium chloride on the dissolution of quartz between pH 1.4 and 12.3 and proposed the following mechanism. In an alkaline environment, negatively charged silicon surfaces dominate according to Helmut et al. [5]. The sodium ions with their solvation shells are drawn towards the surface where the surface complexes  $\equiv\text{SiO}^-$  are protonated by the water molecules in the shells (Fig. 12). Thus  $\text{OH}^-$  ions form directly at the surface locally enhancing  $\text{SiO}_2$  solubility. At pH > 6, more and more surface

**Fig. 12** Schematic diagram of  $\text{SiO}_2$  dissolution in alkaline solutions in the presence of sodium ions (based on [12, 27])



complexes  $\equiv\text{SiO}^--\text{Na}^+$  are expected which are, according to Dove [33] and Dove and Elston [27], associated with faster  $\text{SiO}_2$  dissolution rates.

This effect can explain how sufficient silicon solubility for damaging ASR is achieved at relatively low  $\text{OH}^-$  concentrations in the presence of NaCl. It should be remembered that ASR usually occurs in concrete whose pore solution has a high pH (>13.5). Based on the results of Dove [33] and Dove and Elston [27] the dissolution mechanisms of silicon in concrete containing reactive aggregates exposed to NaCl is summarized below (Fig. 12).

In order to study the effect NaCl on silicon solubility of the present concrete specimens (at pH >12.3) in more detail, simplified solubility equilibria in contrast to the ion-rich concrete pore solution were computed with the hydrogeochemical simulation program PHREEQC [34] using the LLNL database with which the activity coefficients are specified by the WATEQ Debye Hückel equation. Leemann et al. [35] observed that silica dissolution is also controlled by the amount of portlandite in contact with alkaline solutions. Thus the solubility of amorphous  $\text{SiO}_2$  was calculated for a range of KOH solutions buffered, as in the real pore solution, by excess portlandite (to avoid depletion), Fig. 13.

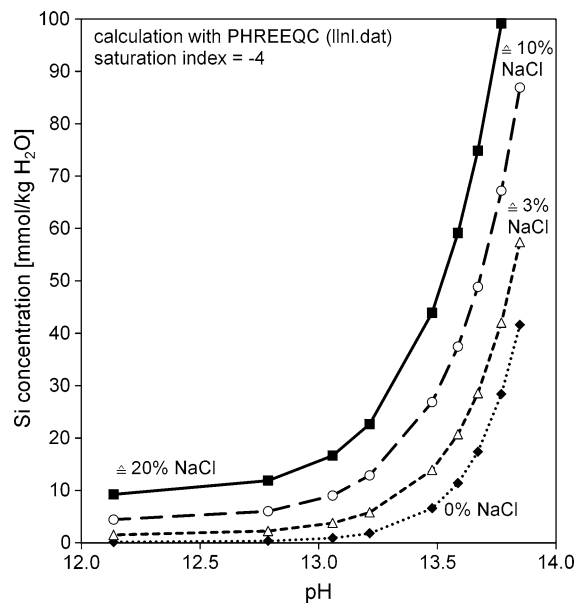


**Fig. 13** Effect of NaCl concentration on silicon solubility in the model system; calculations with PHREEQC on the solubility of amorphous  $\text{SiO}_2$  in KOH solution in the presence of excess portlandite (database: llnl.dat)

In order to obtain realistic silicon concentrations near those measured for the pore solution in concrete at the end of the moist pre-storage period (e.g. HA

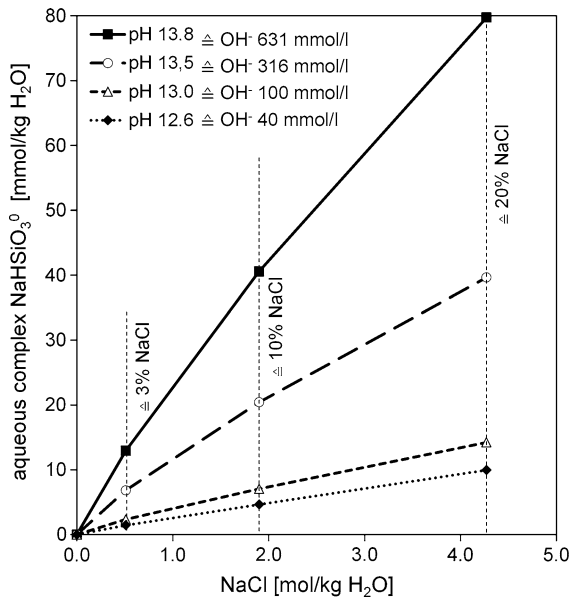


**Fig. 14** Effect of NaCl concentration on formation of an aqueous complex  $\text{NaHSiO}_3^0$  in the model system; calculations with PHREEQC on the solubility of amorphous  $\text{SiO}_2$  in KOH solution in the presence of excess portlandite (database: lnl.dat)

cement 0 % NaCl: pH 13.5; 3 mmol/L Si, Figs. 4, 7) the target saturation index was set to  $-4$ , i.e. the solubility of amorphous  $\text{SiO}_2$  given in the database was, in effect, reduced from  $10^{-2.74}$  to  $10^{-6.74}$  mol/kg  $\text{H}_2\text{O}$ . The reduced saturation index accounts for the removal of Si from the pore solution by the ASR gel. Different amounts of NaCl were then added to the solutions yielding silicon solubility curves as a function of pH and NaCl concentration. Although the calculation becomes increasingly inaccurate at ionic strengths above one, i.e. NaCl concentrations above roughly 6 wt%, the data reveal a general increase in the solubility of silicon with NaCl concentration in approximate agreement with the experimental observations (e.g. HA cement 20 % NaCl: pH 13.0; 11 mmol/L Si, Figs. 4, 7). Thus, as observed in the present experiments, silicon solubility is shifted to a lower pH in the presence of dissolved NaCl. This would mean that silicate minerals become more sensitive to ASR on NaCl ingress.

According to the simulation results, the solubility of silicon is enhanced by the formation of an aqueous complex  $\text{NaHSiO}_3^0$  which increases in concentration with pH and the amount of dissolved NaCl (Fig. 14). This effect and the general decrease in activity of the

aqueous silicate species produced by dissolved NaCl increase the solubility of silicon significantly. Moreover, the complex could be a precursor to the formation of alkali silica gel.

#### 4 Conclusions

Up to now the question whether damaging ASR in concrete is promoted by penetrating NaCl and which mechanisms can occur has not been adequately resolved. The effect of the exposure of concrete containing reactive siliceous aggregate to NaCl solutions on the chemical composition of the pore solution and expansion due to ASR has been investigated. Changes in pore solution composition due to the reaction of dissolved NaCl with the hydration products were studied in storage experiments with hardened cement paste powders stored in artificial pore solutions containing NaCl. Based on the present experimental results and model calculations, the following conclusions were drawn for the effect of chloride ingress on ASR in concrete.

- The penetration of sodium and chloride ions causes a significant increase in expansion and ASR damage of concrete exposed to NaCl solutions.
- The use of low-alkali cements cannot inhibit damaging ASR due to NaCl exposure in all cases.
- The  $\text{OH}^-$  concentration, and therefore pH, of the concrete pore solution is mainly lowered by potassium leaching. The  $\text{OH}^-$  concentration is also lowered by the formation of Friedel's salt from ettringite. Sulphate is released and portlandite is formed accordingly.
- Despite a lower  $\text{OH}^-$  concentration, the Si concentration in the pore solution increases in the presence of dissolved NaCl. Probable causes are the reaction of protons in the solvation shell of the sodium ions with the  $\text{SiO}_2$  surface, the formation of an aqueous  $\text{NaHSiO}_3^0$  complex and the reduction in activity of the aqueous species because dissolved NaCl increases ionic strength.
- The aqueous complex  $\text{NaHSiO}_3^0$  could be a precursor to the formation of alkali silica gel.
- Chloride binding on hydrated cement phases and the corresponding release of  $\text{OH}^-$  ions does not significantly promote ASR. Decisive for ASR damage in

concrete exposed to external NaCl is the total alkali content in the pore solution. This governs silicon solubility and thus gel formation.

Similar results were obtained for concretes containing natural, inhomogeneous aggregates, e.g. grey-wacke, in earlier investigations by the present author [25]. This indicates that the present conclusions for borosilicate glass are also valid for natural aggregates.

**Acknowledgments** The investigations were financed by the German Research Foundation (HE 3217/12-1).

## References

- Breitenbücher R, Sievering C (2012) Cracking in concrete pavements due to alkali–silica-reactions. In: 10th International conference on concrete pavements, Québec, pp 511–521
- Giebson C, Seyfarth K, Ludwig H-M (2012) Correlation of ASR performance testing for highway pavement concretes with field performance and investigations into boosting the alkali level. In: 14th International conference on alkali aggregate reaction, Austin
- Bérubé MA, Dorion JF, Duchesne J, Fournier B, Vézina D (2003) Laboratory and field investigations of the influence of sodium chloride on alkali–silica reactivity. *Cem Concr Res* 33:77–84
- Chatterji S, Thaulow N, Jensen AD (1987) Studies of alkali–silica reaction, part 4. Effect of different alkali salt solutions on expansion. *Cem Concr Res* 17:777–783
- Helmuth R, Stark D, Diamond S, Moranville-Regourd M (1993) Alkali–silica reactivity: an overview of research. Strategic Highway Research Programm, National Research Council, Washington, DC
- Katayama T, Tagami M, Sarai Y, Izumi S, Hira T (2004) Alkali-aggregate reaction under the influence of deicing salts in the Hokuriku district. *Jpn Mater Charact* 53:105–122
- Kawamura M, Arano N, Katafuta K (2000) ASR gel composition, secondary ettringite formation and expansion of mortars immersed in NaCl solution. In: 11th International conference on alkali-aggregate reaction, Québec, pp 199–208
- Sibbick RG, Page CL (1996) Effects of sodium chloride on the alkali–silica reaction in hardened concrete. In: 10th International conference on alkali-aggregate reaction, Melbourne, pp 822–829
- Sibbick RG, Page CL (1998) Mechanisms affecting the development of alkali–silica reaction in hardened concretes exposed to saline environments. *Magn Concr Res* 50:147–159
- Swamy RN (1992) The alkali–silica reaction in concrete. Blackie and Son Ltd, London
- West G (1996) Alkali-aggregate reaction in concrete roads and bridges. Thomas Telford Publications, London
- Iler RK (1979) The chemistry of silica. Wiley, London
- Efes Y (1980) Porengrößenverteilung von Mörteln nach Lagerung im Wasser und in einer Chloridlösung. *Cem Concr Res* 10:231–242
- Hoffmann DW (1984) Changes in structure and chemistry of cement mortars stressed by a sodium chloride solution. *Cem Concr Res* 14:49–56
- Taylor HFW (1997) Cement chemistry, 2nd edn. Thomas Telford Service Ltd, London
- Balonis M, Lothenbach B, Le Saout G, Glasser FP (2010) Impact of chloride on the mineralogy of hydrated Portland cement systems. *Cem Concr Res* 40:1009–1022
- Birmin-Yauri UA, Glasser FP (1998) Friedel’s salt,  $\text{Ca}_2\text{Al}(\text{OH})_6(\text{Cl}, \text{OH})_2\text{H}_2\text{O}$ : its solid solutions and their role in chloride binding. *Cem Concr Res* 28:1713–1723
- Brown P, Bothe J (2004) The system  $\text{CaO}-\text{Al}_2\text{O}_3-\text{CaCl}_2-\text{H}_2\text{O}$  at  $23 \pm 2^\circ\text{C}$  and the mechanisms of chloride binding in concrete. *Cem Concr Res* 34:1549–1553
- Suryavanshi AK, Scantlebury JD, Lyon SB (1996) Mechanism of Friedel’s salt formation in cements rich in tricalcium aluminate. *Cem Concr Res* 26:717–727
- Chatterji S, Jensen AD, Thaulow N, Christensen P (1986) Studies of alkali–silica reaction, part 3. Mechanisms by which NaCl and  $\text{Ca}(\text{OH})_2$  affect the reaction. *Cem Concr Res* 16:246–254
- ASTM C441-05 (2005) ASTM International, West Conshohocken
- Lane D, Ozyildirim H (1999) Evaluation of the effect of Portland cement alkali content, fly ash, ground slag, and silica fume on alkali–silica reactivity. *Cem Concr Aggreg* 21:126–140
- Giebson C (2013) Die Alkali-Kieselsäure-Reaktion in Beton für Fahrbahndecken und Flugbetriebsflächen unter Einwirkung alkalihaltiger Enteisungsmittel. Dissertation, Bauhaus Universität Weimar
- Giebson C, Seyfarth K, Stark J (2010) Influence of acetate and formate-based deicers on ASR in airfield concrete pavements. *Cem Concr Res* 40:537–545
- Dressler A (2013) Effect of de-icing salt and pozzolanic, aluminous supplementary cementitious materials on the mechanisms of damaging alkali–silica reaction in concrete. Dissertation, Technische Universität München
- Herr R, Wieker W (1992) The hydroxide-sulfate ion equilibrium in cement paste pore solutions and its significance to the theory of AAR in concrete. In: 9th International conference on alkali-aggregate reaction in concrete, London, pp 440–450
- Dove PM, Elston SF (1992) Dissolution kinetics of quartz in sodium chloride solutions: analysis of existing data and a rate model for  $25^\circ\text{C}$ . *Geochim Cosmochim Acta* 56:4147–4156
- Jones MR, Macphee DE, Chudek JA, Hunter G, Lannegrand R, Talero R, Scrimgeour SN (2003) Studies using  $^{27}\text{Al}$  MAS NMR of  $\text{AF}_m$  and  $\text{AF}_t$  phases and the formation of Friedel’s salt. *Cem Concr Res* 33:177–182
- Lindgård J, Sellevold EJ, Thomas MDA, Pedersen B, Justnes H, Rønning TF (2013) Alkali–silica reaction (ASR)—performance testing: influence of specimen pre-treatment, exposure conditions and prism size on concrete porosity, moisture state and transport properties. *Cem Concr Res* 53:145–167
- Lindgård J, Thomas MDA, Sellevold EJ, Pedersen B, Andiç-Çakır Ö, Justnes H, Rønning TF (2013) Alkali–silica reaction (ASR)—performance testing: influence of specimen pre-treatment, exposure conditions and prism size on alkali leaching and prism expansion. *Cem Concr Res* 53:68–90



31. Thaulow N, Geiker MR (1992) Determination of the residual reactivity of alkali silica reaction in concrete. In: 9th International conference on alkali-aggregate reaction in concrete, London, pp 1050–1058
32. Wieker W, Herr R (1989) Zu einigen Problemen der Chemie des Portlandzements. *Zeitschrift für Chemie* 29:321–327
33. Dove PM (1994) The dissolution kinetics of quartz in sodium chloride solutions at 25 to 300 °C. *Am J Sci* 294:665–712
34. Parkhurst DL, Appelo CAJ (1999) User's guide to PHREEQC (version 2)—a computer program for speciation, reaction-path, 1D-transport, and inverse geochemical calculations. US Geological Survey Water-Resources Investigations Report 99-4259
35. Leemann A, Le Saout G, Winnefeld F, Rentsch D, Lothenbach B (2011) Alkali–silica reaction: the influence of calcium on silica dissolution and the formation of reaction products. *J Am Ceram Soc* 94:1243–1249